

Correlation Enhanced Autonomous Quantum Battery Charging via Structured Reservoirs

A. Khoudiri,^{1,*} K. El Anouz,^{1,†} and A. El Allati^{1,‡}

¹*Laboratory of R&D in Engineering Sciences, Faculty of Sciences and Techniques Al-Hoceima, Abdelmalek Essaadi University, Tetouan, Morocco.*

We study the charging dynamics of a quantum battery coupled to a structured reservoir composed of two qubits, each in thermal equilibrium with its own bosonic bath. The structured reservoir interacts with a charger–battery model through three distinct configurations: (I) direct coupling between the reservoir qubits and the battery, (II) common coupling between the reservoir qubits, the charger, and the battery, and (III) common coupling between the reservoir qubits and the charger, together with a local charger–battery interaction. For both incoherent and coherent initial states, we analyze the stored energy, ergotropy, and charging power of the battery, and establish upper and lower bounds on the maximum extractable work of the battery based on the free energy of coherence, and exchanged correlations between the subsystems. Our results show that the nature of the interaction scenario and the presence of coherence crucially determine the efficiency of charging and the maximum ergotropy. We demonstrate that correlation exchange between subsystems, quantified by the difference between global and local coherence, acts as a resource for work extraction. These findings provide a deeper understanding of coherence and population and structured environments as resources for autonomous quantum batteries, and offer experimentally accessible predictions within the regime of superconducting qubits.

PACS numbers: 05.70.Ln, 05.30.-d 03.67.-a 42.50.Dv

I. INTRODUCTION

In recent years, the world has become increasingly interested in quantum technology applications [1, 2]. Quantum batteries are one of the most important potential applications in the context of quantum systems [3, 4]. The quantum battery has been studied in many contexts. Farina *et al.* presented a model of a quantum battery based on coherence driving of the quantum battery in contact with a thermal reservoir, in many examples of battery and charger situations [5]. Andolina *et al.* analyzed different classifications and different combinations of quantum harmonic oscillator batteries in the context of charger-mediated energy transfer [6]. Moreover, other contexts have been studied, including the performance of quantum batteries in the context of superconducting qubits [7] and topological quantum batteries under the investigation of the Zeno effect [8].

Engineered reservoirs for coherence-driven optimal charging of quantum batteries are discussed in [9]. The effect of non-Markovian dynamics in the case of strong coupling limits on the optimal charging of a quantum battery with engineered reservoirs is discussed in [10]. We note that in all these papers, only one type of interaction is considered, namely reservoir–charger–battery, where the reservoir–charger is treated as a structured reservoir, and the presence of external work to assist the charging is considered as coherence-driven charging [11–14].

In our framework, we consider a theoretical model of a structured reservoir with two qubits, each qubit being in thermal equilibrium with its reservoir. These qubits interact with a charger–battery model. We investigate the Hilbert space structure of the structured reservoir qubits, the charger, and the battery to analyze three different scenarios: direct coupling between the structured reservoir qubits and the battery; common coupling between the structured reservoir qubits, the charger, and the battery; and common coupling between the structured reservoir qubits and the charger with local interaction between the charger and the battery. We analyze these three scenarios in two contexts of the initial state: a coherent initial state and an incoherent initial state. Moreover, we study the effect of the structured reservoir and each scenario on the charging process using the ergotropy, stored energy, and charging power of the quantum battery. We also provide, theoretically, the bound on the ergotropy based on the free energy stored in the coherence of the subsystems of our theoretical model. Furthermore, we present numerical constraints on each scenario as well as the bounds in each case of the battery ergotropy.

This is what makes our work different from other papers [6–14]. We study the effect of structured reservoirs with their qubits on the charger–battery system. Our model allows the quantum battery to be charged autonomously in each scenario, without any external work. Furthermore, we investigate coherence, population, and the Hilbert space structure as quantum resources for the charging of the quantum battery in each scenario.

Our study interfaces with a growing literature on quantum batteries, ergotropy, and the resource role of coherence and population. Alimuddin *et al.* studied the effect of the structure of passive states on charging, emphasizing

* khoudiri.achraf@etu.uae.ac.ma

† kelanouz@uae.ac.ma

‡ eabderrahim@uae.ac.ma

ing that the limits of the state depend on extractable work [15]. Francica et al. showed that quantum coherence can affect ergotropy and derived coherence-based bounds [16], while Touil, Çakmak, and Deffner discussed the effect of classical correlations on quantum ergotropy [17]. Biswas et al. further connected ergotropy extraction to free-energy bounds with applications to open-cycle engines [18]. More recently, Castellano et al. generalized the notion of local ergotropy to extended settings, refining how work can be locally extracted in multipartite systems [19].

In addition to the theoretical model of the structured reservoir-charger-battery system, we study theoretically the bounds on the ergotropy and the effect of correlations as a resource for boosting the charging of the quantum battery. We establish upper and lower bounds on the ergotropy in each scenario. This is what makes our work an extension of the ideas in [15–19], where we studied the effect of coherence and the free energy of coherence bounds on ergotropy in connected, rather than isolated, systems.

Our paper is organized as follows: In Sec. II, we discuss the Hamiltonian model and the dynamics of our theoretical framework, as well as the scenarios of interaction between the structured reservoir and the charger-battery system in Sec. II A. The scenarios (I, II, III) are presented in Subsecs. II A 1, II A 2, and II A 3. In Subsec. II B, we analyze the theoretical framework of the charging process, energy storage, and ergotropy of the quantum battery. The free energy of coherence and the bounds on the ergotropy of the quantum battery are discussed in Subsubsec. II B 2. The numerical results are presented in Sec. III, where the stored energy, ergotropy, and charging power are analyzed in Subsec. III A, and the effects of coherence and population on the charging of the battery are examined in Subsec. III B. We conclude with a final discussion and conclusion.

II. THEORETICAL MODEL AND GENERAL FRAMEWORK

The model we are interested in consists of charging a quantum Battery, denoted B , with a quantum charger, denoted C , in the context of a structured reservoir, which consists of qubits S_1 and S_2 connected to bosonic thermal reservoirs R_1 and R_2 , respectively. In our work, we will focus on the system denoted $S = S_1 \otimes S_2 \otimes C \otimes B$, which is defined by the Hamiltonian (with $\hbar = 1$ and $K_B = 1$)

$$\hat{H}_S = \sum_{m=1}^2 \hat{H}_{S_m} + \sum_{n=\{C,B\}} \hat{H}_n + \hat{H}_{Int}, \quad (1)$$

$$\hat{H}_{S_m} = \omega_{S_m} \hat{\sigma}_{S_m}^+ \hat{\sigma}_{S_m}^-, \quad (m = \{1, 2\}), \quad (2)$$

$$\hat{H}_n = \omega_n \hat{\sigma}_n^+ \hat{\sigma}_n^-, \quad (n = \{C, B\}), \quad (3)$$

where \hat{H}_{S_m} and \hat{H}_n are the free Hamiltonians, and ω_{S_m} and ω_n are the energy spacings of the qubits S_m and n , respectively. The raising and lowering operators are defined as $\hat{\sigma}_{[\cdot]}^+ = |1\rangle_{[\cdot]} \langle 0|$ and $\hat{\sigma}_{[\cdot]}^- = |0\rangle_{[\cdot]} \langle 1|$, acting on the computational basis states of the respective qubits.

We investigate the Hamiltonian \hat{H}_{Int} , which describes the interaction between the qubits of the system S . Here, we will discuss three scenarios, as presented in Fig. 1. After analyzing the dynamics of the system S , we will discuss each scenario in the following subsections. The total density matrix, denoted $\hat{\rho}_S(0)$, is given by

$$\hat{\rho}_S(0) = \hat{\rho}_{S_{12}}(0) \bigotimes_{n=\{C,B\}} \hat{\rho}_n(0), \quad (4)$$

where $\hat{\rho}_{S_{12}}(0) = \hat{\rho}_{S_1}(0) \otimes \hat{\rho}_{S_2}(0)$ is the initial state of the structured reservoir qubits S_1 and S_2 , and $\hat{\rho}_n(0)$ is the initial state of the qubits $n = \{C, B\}$. In our treatment, we consider that each qubit S_m is weakly coupled to its reservoir R_m . Since the reservoirs R_1 and R_2 are bosonic thermal reservoirs, the evolution of the total system $\hat{\rho}_S(t)$ is described by the Markovian master equation [20–22] as follows:

$$\frac{d}{dt} \hat{\rho}_S(t) = -i \left[\sum_{m=1}^2 \hat{H}_{S_m} + \sum_{n=\{C,B\}} \hat{H}_n, \hat{\rho}_S(t) \right] + \mathcal{L}_{S_{12}}[\hat{\rho}_S(t)], \quad (5)$$

where $[\cdot, \cdot]$ denotes the usual commutator. The first term in the master equation, Eq. 5, represents the free evolution of the system under its free Hamiltonians and corresponds to the reversible (unitary) evolution of the system S . The second term, $\mathcal{L}_{S_{12}}[\hat{\rho}_S(t)]$, represents both the interaction between the subsystems of S and the dissipative interaction of the qubits S_m with their respective reservoirs R_m . This term accounts for the irreversible (non-unitary) evolution of the total system S and is given by

$$\mathcal{L}_{S_{12}}(t)[\hat{\rho}(t)] = -i [H_{Int}, \hat{\rho}_S(t)] + \sum_{m=1}^2 \mathcal{D}^{[T_{R_m}]}[\hat{\rho}_S(t)], \quad (6)$$

$$\begin{aligned} \mathcal{D}^{[T_{R_m}]}[\hat{\rho}_S(t)] &= \gamma_m (\bar{n}_m(T_{R_m}, \omega_{S_m}) + 1) \mathcal{D}^{[\hat{\sigma}_{S_m}^-]}[\hat{\rho}_S(t)] + \\ &\quad \gamma_m \bar{n}_m(T_{R_m}, \omega_{S_m}) \mathcal{D}^{[\hat{\sigma}_{S_m}^+]}[\hat{\rho}_S(t)], \\ \mathcal{D}^{[\hat{\sigma}_{S_m}^\pm]}[\hat{\rho}_S(t)] &= \hat{\sigma}_{S_m}^\pm \hat{\rho}_S(t) \hat{\sigma}_{S_m}^\mp - \frac{1}{2} \{ \hat{\sigma}_{S_m}^\mp \hat{\sigma}_{S_m}^\pm, \hat{\rho}_S(t) \}, \end{aligned}$$

Here, T_{R_m} for $m = \{1, 2\}$ are the temperatures of the reservoirs, and $\gamma_m \ll \omega_{S_m}$ are the decay rates, which set the timescale of the dissipation. The quantity $\bar{n}_m(T_{R_m}, \omega_{S_m})$ represents the average number of quanta (bosons) in the reservoir R_m , and is given by

$$\bar{n}_m(T_{R_m}, \omega_{S_m}) = \frac{1}{\exp\left(\frac{\omega_{S_m}}{T_{R_m}}\right) - 1}.$$

We consider that the qubits S_m and the reservoirs R_m are coupled at resonance. For simplifying in the rest of article we consider $T_{R_1} = T_{R_2} = T$.

A. Quantum Battery and Structured Reservoir Scenarios

Structured reservoirs allow the study of backflow effects and energy transfer in the battery-charger system with the auxiliary qubits of the structured reservoir [23, 24]. We will investigate the Hilbert space of the system S qubits to realize three scenarios of the interaction \hat{H}_{Int} between the structured reservoir qubits S_{12} and the charger-battery subsystem.

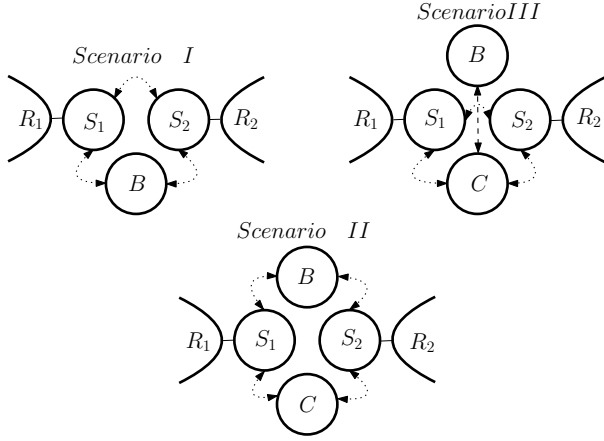


FIG. 1. Schematic representation of the three interaction scenarios between the structured reservoir qubits S_1 and S_2 , the charger C , and the quantum battery B . (a) Scenario I: direct coupling between S_{12} and the B . (b) Scenario II: common coupling between $S_{12}-C-B$ system. (c) Scenario III: common coupling between $S_{12}-C$, together with a local interaction between $C-B$. Each reservoir qubit S_m is in contact with its own bosonic thermal reservoir R_m ($m = 1, 2$).

1. Scenario I: Common interaction between S_{12} and the battery

For this scenario, we consider the battery B to be in direct contact with the qubits S_{12} , as illustrated in Fig. 1 (Scenario I), with the objective of establishing a common interaction between S_1 , S_2 , and B . The goal is to induce transitions from the state $|0_{S_1}1_{S_2}0_B\rangle$ to the state $|1_{S_1}0_{S_2}1_B\rangle$ under the resonance condition between S_{12} and the battery, given by

$$\omega_B = \omega_{S_2} - \omega_{S_1}, \quad \omega_{S_2} > \omega_{S_1}, \quad (7)$$

which physically corresponds to the exchange of excitation between the subsystem qubits $S = S_1 \otimes S_2 \otimes B$. The interaction Hamiltonian for this scenario, denoted \hat{H}_{IntI} , is given by

$$\hat{H}_{IntI} = g_1 [|0_{S_1}1_{S_2}0_B\rangle \langle 1_{S_1}0_{S_2}1_B| + \text{H.c.}], \quad (8)$$

where $g_1 \ll \omega_B$ is the coupling between B and S_{12} . In this configuration, S_{12} acts as a filter for the decoherence

effects of the reservoirs R_1 and R_2 on the quantum battery B , and it is also used in the context of autonomous quantum thermal machines in [25, 26]. In our scenario, this type of interaction enables the battery B to charge autonomously from S_{12} without any external work.

2. Scenario II: Common interaction between S_{12} and the charger-battery system

In this scenario, we analyze the case of a common interaction between S_{12} and C and B , respectively, as illustrated in Fig. 1 (Scenario II). We realize a common interaction between the total system qubits to drive the transition from $|0_{S_1}1_{S_2}1_C0_B\rangle$ to $|1_{S_1}0_{S_2}0_C1_B\rangle$ under the resonance condition

$$\omega_{S_2} - \omega_{S_1} = \omega_C - \omega_B, \quad (9)$$

where $\omega_{S_2} > \omega_{S_1}$ and $\omega_C > \omega_B$, which physically corresponds to the exchange of excitation between the total system qubits S . In this scenario, S_{12} filters the decoherence effects of R_1 and R_2 on the charger-battery system. The interaction Hamiltonian, denoted \hat{H}_{IntII} , is given by

$$\hat{H}_{IntII} = g_2 [|0_{S_1}1_{S_2}1_C0_B\rangle \langle 1_{S_1}0_{S_2}0_C1_B| + \text{H.c.}], \quad (10)$$

where $g_2 \ll (\omega_{S_2} - \omega_{S_1})$ is the coupling between S_{12} and the charger-battery system.

3. Scenario III: Common interaction between S_{12} and the charger, and local charger-battery interaction

We now consider a common interaction between S_{12} and the charger, with the objective of driving the transition from the state $|0_{S_1}1_{S_2}0_C\rangle \langle 0_{S_1}1_{S_2}0_C| \otimes \mathcal{I}_B$ to the state $|1_{S_1}0_{S_2}1_C\rangle \langle 1_{S_1}0_{S_2}1_C| \otimes \mathcal{I}_B$. Between the charger and the battery, the interaction biases the transition $\mathcal{I}_{S_{12}} \otimes |1_C0_B\rangle \langle 1_C0_B|$ to the state $\mathcal{I}_{S_{12}} \otimes |0_C1_B\rangle \langle 0_C1_B|$ under the resonance condition

$$\omega_B = \omega_C = \omega_{S_2} - \omega_{S_1}, \quad \omega_{S_2} > \omega_{S_1}, \quad (11)$$

which physically corresponds to the sequential transfer of energy from S_{12} to the charger, and from the charger to the battery, mediated by the interaction between S_{12} and C . The interaction Hamiltonian, denoted \hat{H}_{IntIII} , is given by

$$\begin{aligned} \hat{H}_{IntIII} = & g_3 [|0_{S_1}1_{S_2}0_C\rangle \langle 1_{S_1}0_{S_2}1_C| + \text{H.c.}] \otimes \mathcal{I}_B \\ & + k \mathcal{I}_{S_{12}} \otimes [|1_C0_B\rangle \langle 0_C1_B| + \text{H.c.}], \end{aligned} \quad (12)$$

where g_3 and k are the respective coupling strengths for the S_{12} -charger and charger-battery interactions. In this case $S_{12} \otimes C$ are filtered the decoherence of R_1 and R_2 into the battery.

In the following sections of the paper, we analyze the effect of each scenario on the charging process, as well as the influence of coherence and memory effects on the maximum work extracted from the battery over time.

B. Charging Process: Stored Energy, Ergotropy, and Contributions from Coherence and Populations

In this section, we analyze the charging process of the quantum battery B in each scenario of our theoretical model, based on the stored energy, ergotropy, and the free energy of coherence of the quantum battery. We also analyze the bounds on the quantum ergotropy of the battery within our theoretical framework.

1. Energy Storage and Ergotropy of the Quantum Battery

The energy stored in the quantum battery B over time, denoted E_B , is an important quantity to highlight the energy transferred to the quantum battery. Mathematically, it is defined as

$$E_B = \text{Tr}\{\hat{H}_B \hat{\rho}_B\}, \quad (13)$$

where this energy can increase over time; however, this does not necessarily mean that the battery is being charged. Physically, it represents only the stored energy. The battery is considered charged only if its state is passive [15], meaning that work can be extracted from it.

To analyze the maximum work extractable from the quantum battery, we use the concept of quantum ergotropy [19], denoted \mathcal{E}_B , which represents the difference between the energy stored and the energy of the quantum battery in its passive state, denoted $E_{B_{\text{Pss}}} = \text{Tr}\{\hat{H}_B \hat{\rho}_{B_{\text{Pss}}}\}$. The ergotropy is mathematically defined as

$$\mathcal{E}_B = E_B - E_{B_{\text{Pss}}}. \quad (14)$$

The passive state of the quantum battery [19], denoted $\hat{\rho}_{B_{\text{Pss}}}$, is defined as follows. Mathematically, the energy of the ground state of the quantum battery is taken as zero, while the energy of the excited state is ω_B . The spectral decomposition of the quantum battery state is given by

$$\hat{\rho}_B = \sum_{i=0}^1 \psi_i |\psi_i\rangle \langle \psi_i|, \quad (15)$$

where $\psi_0(t) \leq \psi_1(t)$ and $|\psi_i\rangle$ are the eigenvalues and eigenvectors of $\hat{\rho}_B$. The corresponding passive state is then

$$\hat{\rho}_{B_{\text{Pss}}} = \sum_{i=0}^1 \psi_i |i\rangle \langle i|. \quad (16)$$

The ergotropy of the battery in Eq. 14, can also consists of two contributions [16–18, 27]. The population ergotropy, denoted \mathcal{E}_B^P , represents the maximal work extractable due to the population distribution of the quantum battery B . The coherence ergotropy, denoted \mathcal{E}_B^C ,

represents the maximal work extractable due to the quantum coherence of the battery. Mathematically, Eq. 14 can be expressed as

$$\mathcal{E}_B = \mathcal{E}_B^P + \mathcal{E}_B^C, \quad (17)$$

where,

$$\mathcal{E}_B^C = \mathcal{E}_B - \mathcal{E}_B^P, \quad (18)$$

$$\mathcal{E}_B^P = E_B - \bar{E}_{B_{\text{Pss}}}, \quad (19)$$

where $\bar{E}_{B_{\text{Pss}}} = \text{Tr}\{\hat{H}_B \bar{\rho}_{B_{\text{Pss}}}\}$ is the energy of the passive state $\bar{\rho}_{B_{\text{Pss}}}$ of the fully dephased state of the quantum battery [28], denoted $\bar{\rho}_B$. Mathematically, it is given by

$$\bar{\rho}_B = \sum_{i=0}^1 \langle i | \hat{\rho}_B | i \rangle |i\rangle \langle i|. \quad (20)$$

For each subsystem, $\bar{\rho}_x$, for $x = \{S_1, S_2 \text{ and } C\}$, this represents the corresponding incoherent state.

2. Free Energy of Coherence and Bounds on Quantum Battery Ergotropy

As demonstrated in Eq. 14, the ergotropy can originate either from the population or from the coherence of the quantum battery. In the literature, the maximum extractable work due to coherence is quantified by the free energy of coherence [17, 18, 28]. For any state $\hat{\rho}$, denoted $W(\hat{\rho})$, it is mathematically defined as

$$W(\hat{\rho}) = F(\hat{\rho}) - F(\bar{\rho}) = K_B T \mathcal{C}(\hat{\rho}), \quad (21)$$

where $F(\hat{\rho})$ and $F(\bar{\rho})$ represent the free energies of the state $\hat{\rho}$ and its fully dephased state $\bar{\rho}$, respectively, and $\mathcal{C}(\hat{\rho})$ is the relative entropy of coherence [30], which quantifies the coherence of $\hat{\rho}$. Mathematically, the free energy of $\hat{\rho}$ is defined as [29]

$$F(\hat{\rho}) = E - K_B T S(\hat{\rho}), \quad (22)$$

where $E = \text{Tr}\{\hat{\rho} \hat{H}\}$ is the energy of $\hat{\rho}$ with Hamiltonian \hat{H} , and $S(\hat{\rho}) = -\text{Tr}\{\hat{\rho} \log_2 \hat{\rho}\}$ is the von Neumann entropy. Here, T denotes the reservoir temperature and K_B is the Boltzmann constant.

For $\mathcal{C}(\hat{\rho})$, the relative entropy of coherence is mathematically defined as [30]

$$\mathcal{C}(\hat{\rho}) = S(\bar{\rho}) - S(\hat{\rho}). \quad (23)$$

In our scenario, we note that the free energy of coherence of the quantum battery, $W(\hat{\rho}_B)$, bounds the ergotropy of coherence, Eq. 18, such that

$$0 \leq \mathcal{E}_B^C \leq W(\hat{\rho}_B) := K_B T \mathcal{C}(\hat{\rho}_B), \quad (24)$$

which physically means that the maximal extractable work from coherence is bounded by the free energy of

coherence. This represents the maximum work stored in the coherence, indicating that we cannot extract the full energy from coherence due to the decoherence effect of the reservoir.

Using Eqs. 17 and 24, we obtain that the total ergotropy of the quantum battery is also bounded as

$$\mathcal{E}_B^P \leq \mathcal{E}_B \leq K_B T \mathcal{C}(\hat{\rho}_B) + \mathcal{E}_B^P, \quad (25)$$

where we have two bounds on the quantum battery ergotropy. This means that the minimal value of the ergotropy is $\min \mathcal{E}_B = \mathcal{E}_B^P$ and the maximal value is $\max \mathcal{E}_B = K_B T \mathcal{C}(\hat{\rho}_B) + \mathcal{E}_B^P$. Note that if the ergotropy of the population is zero, the ergotropy is bounded between $\min \mathcal{E}_B = 0$ and $\max \mathcal{E}_B = K_B T \mathcal{C}(\hat{\rho}_B)$. These results are also provided in [17, 18, 28], which give the upper and lower bounds of the ergotropy.

Moreover, we can give a general bound on the ergotropy of the quantum battery based on the total relative entropy of the system S . The free energy of coherence of the total system S is given by

$$W(\hat{\rho}_S) = K_B T \mathcal{C}(\hat{\rho}_S), \quad (26)$$

using Eq. 23. The conventional mutual information [31] of the total system S , denoted I_S , describes the correlations (quantum and classical) between the subsystems S_1 , S_2 , C , and B , and is mathematically defined as

$$I_S = \sum_{m=1}^2 S(\hat{\rho}_{S_m}) + \sum_{n=\{C,B\}} S(\hat{\rho}_n) - S(\hat{\rho}_S), \quad (27)$$

so that the free energy of coherence of the total system S can now be expressed as

$$W(\hat{\rho}_S) = K_B T \left(\sum_{m=1}^2 \mathcal{C}(\hat{\rho}_{S_m}) + \sum_{n=\{C,B\}} \mathcal{C}(\hat{\rho}_n) + I_S - \bar{I}_S \right), \quad (28)$$

where we observe that the total free energy of coherence of the total system is given as the sum of the free energy of coherence of each subsystem, $K_B T \sum_{m=1}^2 \mathcal{C}(\hat{\rho}_{S_m})$ and $\sum_{n=\{C,B\}} \mathcal{C}(\hat{\rho}_n)$, plus the difference between the total and global relative entropy of coherence of the total system, $I_S - \bar{I}_S$, which is defined as

$$\begin{aligned} \Delta C(\hat{\rho}_S) &= \mathcal{C}(\hat{\rho}_S) - \sum_{m=1}^2 \mathcal{C}(\hat{\rho}_{S_m}) - \sum_{n=\{C,B\}} \mathcal{C}(\hat{\rho}_n), \\ &= I_S - \bar{I}_S. \end{aligned} \quad (29)$$

Here, $\Delta C(\hat{\rho}_S)$ represents the difference between the total and global relative entropy of coherence of the total system S , and \bar{I}_S is the conventional mutual information of the fully dephased state of the total system S , describing the correlations due to the populations in the subsystems of S . This is also provided in [17, 18], where the mutual information is used because only two subsystems are

studied. In our case, we use the conventional mutual information because we study four interacting subsystems. $\Delta C(\hat{\rho}_S)$ demonstrates that the ergotropy in our battery is affected by the total correlation exchange between the subsystems of S .

III. RESULTS AND DISCUSSION

In this section, we numerically study our theoretical model to analyze the charging process in each scenario (I, II, and III), as well as the effect of coherence and population on the maximum extractable work over time. We study two examples of initial states for each model and make a comparison between them.

In the first example, denoted for each scenario as (I_a , II_a , III_a), we consider the initial state of the total system S as

$$\hat{\rho}_{S_a}(0) = |0_{S_1} 1_{S_2} 0_B\rangle \quad \text{for scenario } I_a,$$

and

$$\hat{\rho}_{S_a}(0) = |0_{S_1} 1_{S_2} 1_C 0_B\rangle \quad \text{for scenarios } (II_a \text{ and } III_a).$$

In the second example, denoted for each scenario as (I_b , II_b , III_b), we consider for S_{12} the state

$$|\psi_{S_{12}}(0)\rangle = \frac{1}{\sqrt{2}} \left[|0_{S_1} 1_{S_2}\rangle + |1_{S_1} 0_{S_2}\rangle \right],$$

for the charger

$$|\psi_C(0)\rangle = \frac{1}{\sqrt{2}} \left[|0_C\rangle + |1_C\rangle \right],$$

and for the battery

$$|\psi_B(0)\rangle = |0_B\rangle,$$

where the total initial state for for scenario I_a

$$\hat{\rho}_{S_b}(0) = |\psi_{S_{12}}(0)\psi_B(0)\rangle \langle \psi_{S_{12}}(0)\psi_B(0)|,$$

and the total initial state for for scenarios (II_a and III_a)

$$\hat{\rho}_{S_b}(0) = |\psi_{S_{12}}(0)\psi_C(0)\psi_B(0)\rangle \langle \psi_{S_{12}}(0)\psi_C(0)\psi_B(0)|,$$

. The example S_a highlights the effect of population on the charging process, since the initial state is incoherent, while the example S_b highlights the effect of coherence on the charging process. For each example, the battery is initially in a non-passive state, with zero initial energy.

In our numerical simulation, we set the energy spacing of qubit S_2 to $\omega_{S_2} = 10$, and for the other parameter, we used $\omega_{S_1} = 0.5\omega_{S_2}$. The reservoir temperatures were set as $T_{R_1} = T_{R_2} = T = \omega_{S_1}$, and the decay rate was chosen as $\gamma_m = 0.01\omega_{S_m}$ for $m = \{1, 2\}$.

We focus on analyzing the coupling between S_{12} and the charger-battery system. Throughout the rest of the paper, the coupling g takes the values 0.03, 0.05,

0.07, and 0.09 in units of ω_{S_2} , which are represented in the plots by red (dotted), black (dashed), blue (dotted-dashed), and magenta (solid) lines. For scenario III, the coupling between the charger and the battery is set to $0.03\omega_C$.

For these parameters, the condition $g/\omega_{S_2} \leq 0.1$ is satisfied, which corresponds to the weak coupling limit. Experimentally, this lies within the range of superconducting qubits, where ω_{S_2} is in the order of GHz, while the couplings g and k are in the order of MHz, and the time scale is in the range of μs – ms . This shows that our theoretical model can be experimentally realized using superconducting qubits [31–34].

A. Charging Process

In this section, we manipulate numerically the ergotropy Eq. 14 and the energy Eq. 13 of the quantum battery over time. Also, we define the charging power of the battery over time [35], denoted $\mathcal{P}_B(t)$, which is mathematically defined as

$$\mathcal{P}_B(t) = \frac{\mathcal{E}_B(t)}{t}, \quad (30)$$

and describes how fast the quantum battery becomes extractably charged over time. Note that we use the normalized quantities, $\frac{\mathcal{E}_B(t)}{\omega_B}$, $\frac{E_B(t)}{\omega_B}$, and $\frac{\mathcal{P}_B(t)}{\omega_B}$, to compare correctly between the three scenarios in the two examples of the initial states.

For scenarios (I_a, II_a, III_a) and (I_b, II_b, III_b) in Figs. (2a, 2b, 2c) and Figs. (2d, 2e, 2f), we observe that for $(I_{a,b}, II_{a,b})$, the ergotropy, the energy, and the charging power increase over time as the coupling g increases. In contrast, for $(III_{a,b})$, they increase as g decreases over time.

Physically, for $(I_{a,b}, II_{a,b})$, the interaction is common between $S_{12}B$ and $S_{12}CB$, and according to the interaction Hamiltonians of the scenarios $(I$ and $II)$ in Eq. 8 and Eq. 10, respectively, they bias the transitions

$$\begin{aligned} |0_{S_1}1_{S_2}0_B\rangle &\rightarrow |1_{S_1}0_{S_2}1_B\rangle \quad \text{for Scenario I,} \\ |0_{S_1}1_{S_2}1_C0_B\rangle &\rightarrow |1_{S_1}0_{S_2}0_C1_B\rangle \quad \text{for Scenario II,} \end{aligned}$$

which means that the quantum battery is transferred from the non-passive state $|0_B\rangle$ to the fully passive state $|1_B\rangle$ for the two scenarios $(I$ and $II)$. In contrast, in scenario (III) , the transition of the quantum battery from the non-passive state to the fully passive state occurs immediately via the quantum charger.

We also observe that the ergotropy, the energy, and the charging power decrease when transitioning from (I_a, II_a, III_a) to (I_b, II_b, III_b) , which means that the battery transfers to the passive state in (I_a, II_a, III_a) more efficiently than in (I_b, II_b, III_b) . We analyze why the battery transfers to the passive state in (I_a, II_a, III_a) more efficiently than in (I_b, II_b, III_b) in the next section, where we study the effect of population and coherence on the charging of the quantum battery over time.

B. Effects of coherence and population on the charging process

In this section, we study numerically the effect of coherence and population on the charging process of the quantum battery. We analyze the coherence transfer between the external subsystems of the total system S over time, as well as the correlation exchange using the difference between the global and local coherence of S , Eq. 29. Note that the analysis of coherence is similar to the analysis of the free energy of coherence of each subsystem S_{12} , C , B , and the total system S , according to Eq. 21 and Eq. 28.

For scenarios (I_a, II_a, III_a) in Figs. (3a, 3b, 3c), we observe that the coherence

$$\mathcal{C}(\hat{\rho}_{S_{12}}(t)) = \mathcal{C}(\hat{\rho}_C(t)) = \mathcal{C}(\hat{\rho}_B(t)) = 0$$

of each subsystem S_{12} , C , and B is zero over time. Physically, this means that the free energy extractable from the coherence of each subsystem is zero,

$$W(\hat{\rho}_{S_{12}}(t)) = W(\hat{\rho}_C(t)) = W(\hat{\rho}_B(t)) = 0.$$

Only the total exchanged correlation, $\Delta\mathcal{C}(t)$, increases non-monotonically over time, which physically implies that the total free energy of coherence in this scenario is due to the correlation exchange, i.e.,

$$W(\hat{\rho}_S) = K_B T \Delta\mathcal{C}(t).$$

For scenarios (I_b, II_b, III_b) in Figs. (3d, 3e, 3f), we observe that the coherences $\mathcal{C}(\hat{\rho}_{S_{12}}(t))$ and $\mathcal{C}(\hat{\rho}_C(t))$ are initially maximal and decrease over time, while $\mathcal{C}(\hat{\rho}_B(t))$ is initially zero and increases over time. Physically, this indicates a transfer of coherence between the subsystems of S , so that free energy can be extracted from the coherence of S_{12} and C into B . In addition, the correlation $\Delta\mathcal{C}(t)$ increases, which means that Eq. 28 can be interpreted for scenario (I_b) as

$$W(\hat{\rho}_B(t)) = W(\hat{\rho}_S(t)) - W(\hat{\rho}_{S_{12}}(t)) - K_B T \Delta\mathcal{C}(t),$$

and for scenarios (II_b, III_b) as

$$W(\hat{\rho}_B(t)) = W(\hat{\rho}_S(t)) - W(\hat{\rho}_{S_{12}}(t)) - W(\hat{\rho}_C(t)) - K_B T \Delta\mathcal{C}(t).$$

Physically, this means that coherence is being charged into B from S_{12} and C over time. The non-monotonic evolution of $\Delta\mathcal{C}(t)$ for all scenarios (I_a, II_a, III_a) and (I_b, II_b, III_b) is due to the memory effect and the back-flow of information between the subsystems of S over time. Here, $\Delta\mathcal{C}(t) = I_S(t) - \bar{I}_S(t)$ also describes the correlation exchanged between the subsystems. The non-Markovianity arises from the exchange of correlations between the subsystems in the case of structured reservoirs [26].

These results of the free energy of coherence directly affect the variation of ergotropy, Eq. 17, where the total ergotropy consists of two parts: one due to coherence

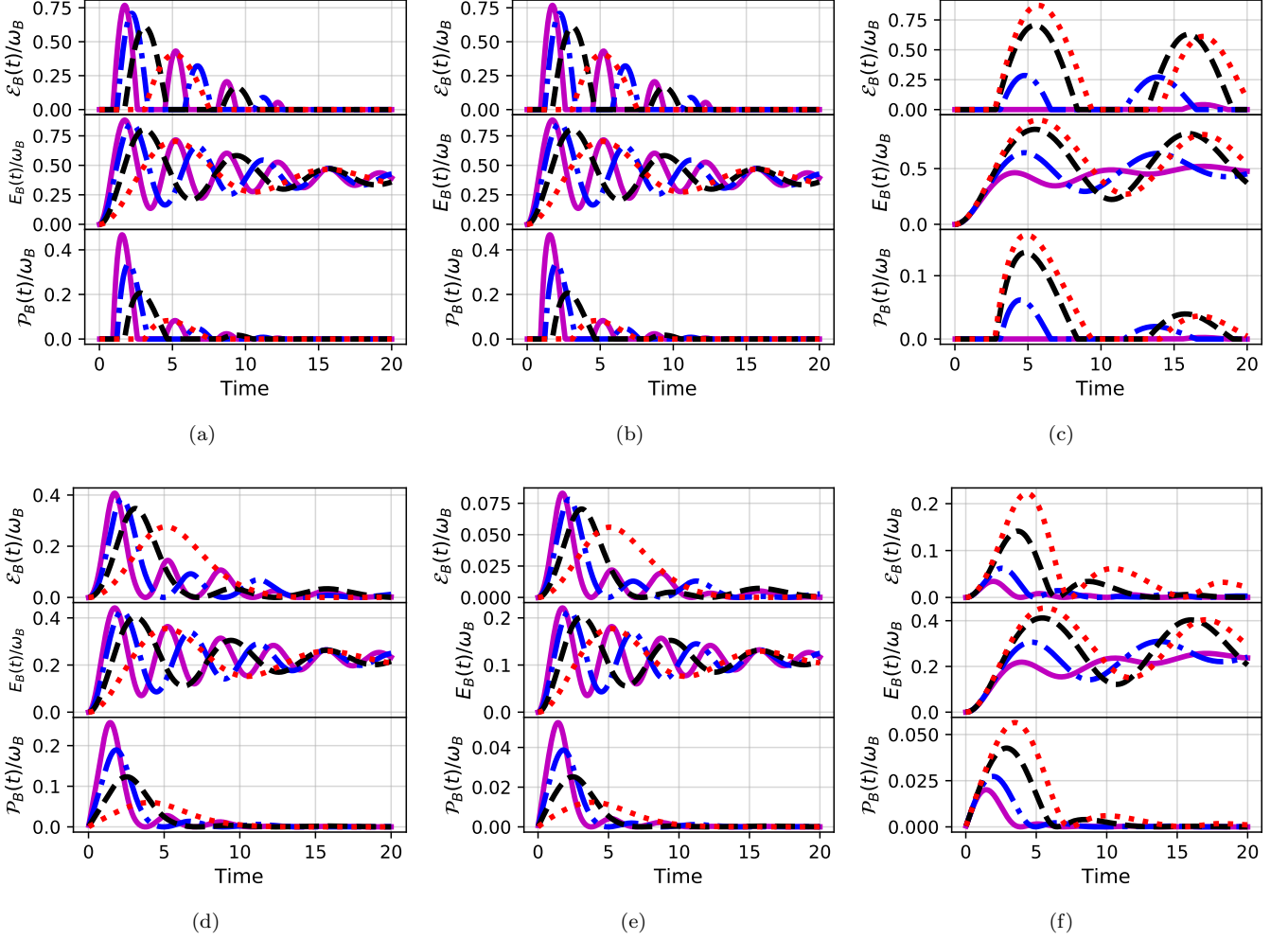


FIG. 2. Time evolution of $\frac{\mathcal{E}_B(t)}{\omega_B}$, $\frac{E_B(t)}{\omega_B}$, and $\frac{\mathcal{P}_B(t)}{\omega_B}$, representing the ergotropy, energy, and charging power of the quantum battery, respectively. Panels (a)–(c) correspond to scenarios (I_a , II_a , III_a), while panels (d)–(f) correspond to scenarios (I_b , II_b , III_b). The coupling strength is varied as $g = 0.03, 0.05, 0.07$, and 0.09 (in units of ω_{S_2}), represented by red (dotted), black (dashed), blue (dot-dashed), and magenta (solid) curves.

and the other due to population. Here, we analyze the effect of the ergotropy of coherence and the ergotropy of population over time, denoted by $\mathcal{E}_B^C(t)$ and $\mathcal{E}_B^P(t)$, respectively.

For scenarios (I_a , II_a , III_a) in Figs. (4a, 4b, 4c), we observe that the ergotropy of coherence is zero over time, while the ergotropy of population increases over time. In connection with the free energy of coherence shown in Figs. (3a, 3b, 3c), the coherence energies for each subsystem S_{12} , C , and B remain zero over time. According to Eq. 25, this can now be interpreted as

$$\mathcal{E}_B^P(t) \leq \mathcal{E}_B(t) \leq \mathcal{E}_B^P(t),$$

which physically means that the ergotropy for scenarios (I_a , II_a , III_a) is due only to the population, i.e.,

$$\mathcal{E}_B(t) = \mathcal{E}_B^P(t),$$

under the exchange of the total correlations between the subsystems of S .

For scenarios (I_b , II_b , III_b) in Figs. (4d, 4e, 4f), we observe that the ergotropy of population is zero, while the ergotropy of coherence increases over time. According to the bound of ergotropy Eq. 25, this can now be interpreted as follows:

For scenario (I_b):

$$0 \leq \mathcal{E}_B(t) \leq W(\hat{\rho}_S(t)) - W(\hat{\rho}_{S_{12}}(t)) - K_B T \Delta \mathcal{C}(t),$$

For scenarios (II_b , III_b):

$$0 \leq \mathcal{E}_B(t) \leq W(\hat{\rho}_S(t)) - W(\hat{\rho}_{S_{12}}(t)) - W(\hat{\rho}_C(t)) - K_B T \Delta \mathcal{C}(t),$$

Physically, this means that the maximal values of ergotropy $\mathcal{E}_B(t)$ are smaller than $W(\hat{\rho}_S(t)) - W(\hat{\rho}_{S_{12}}(t)) - W(\hat{\rho}_C(t)) - K_B T \Delta \mathcal{C}(t)$ and depend directly on the free

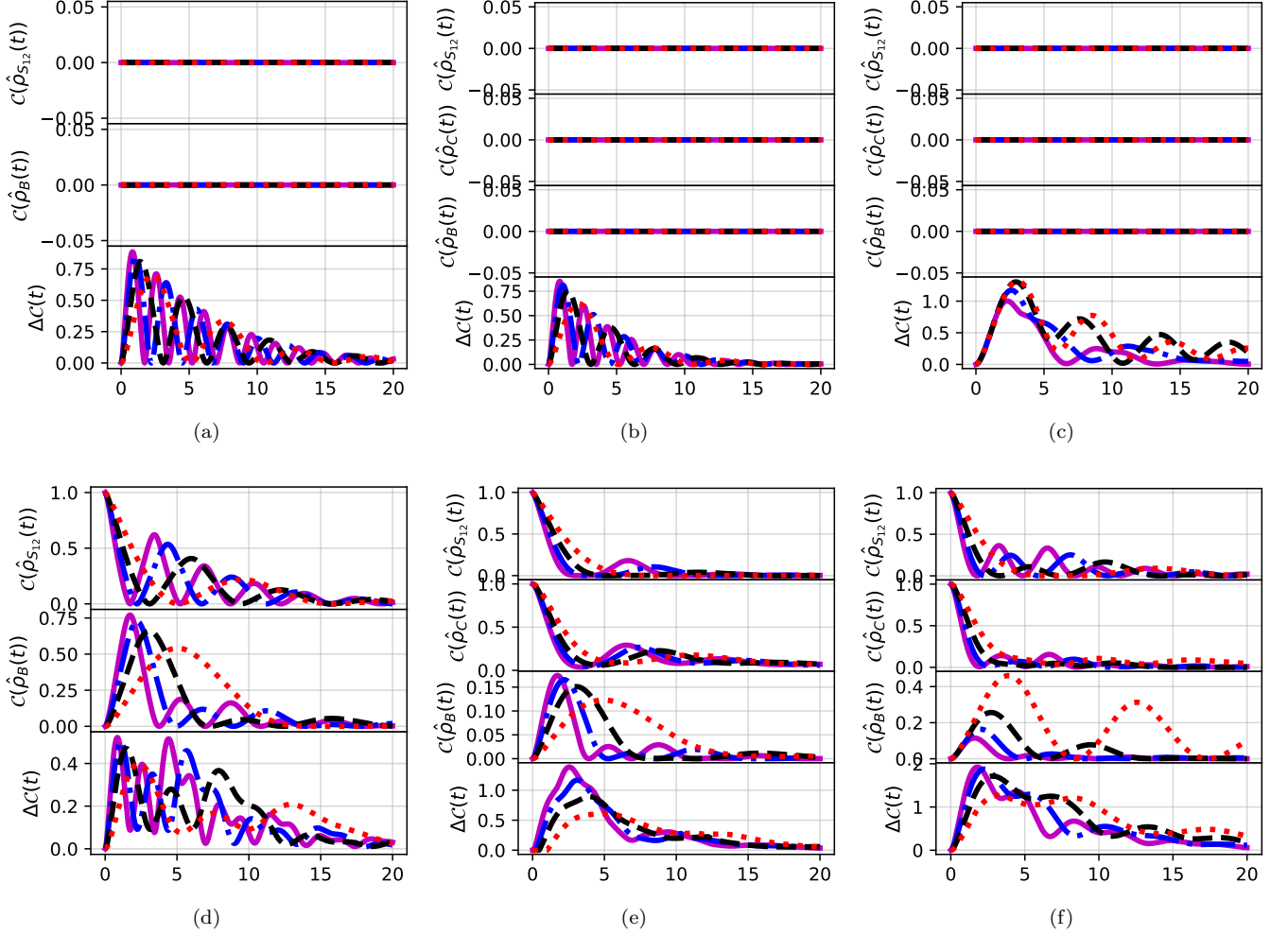


FIG. 3. Time evolution of $\mathcal{C}(\hat{\rho}_{S_{12}}(t))$, $\mathcal{C}(\hat{\rho}_C(t))$, $\mathcal{C}(\hat{\rho}_B(t))$ and $\Delta\mathcal{C}(t)$, representing the relative entropy of coherence of the S_{12} , C , B and difference between local and global coherence of S , respectively. Panels (a)–(c) correspond to scenarios (I_a, II_a, III_a) , while panels (d)–(f) correspond to scenarios (I_b, II_b, III_b) . The coupling strength is varied as $g = 0.03, 0.05, 0.07$, and 0.09 (in units of ω_{S_2}), represented by red (dotted), black (dashed), blue (dot-dashed), and magenta (solid) curves.

energies of coherence of the subsystems S_{12} , C , and the total system S .

The difference between the ergotropy bounds in scenarios (I_a, II_a, III_a) and (I_b, II_b, III_b) explains why the ergotropy in (I_a, II_a, III_a) is larger than in (I_b, II_b, III_b) over time.

C. Discussion

Our model integrates structured reservoirs and explicitly compares three distinct interaction scenarios between the reservoir qubits S_{12} , the charger C , and the battery B . This analysis allows us to delineate how structured reservoir, the backflow of information, and the correlation exchange between the total system S qubits govern charging and work extraction, going beyond analyses that treat coherence, population, or correlations in isola-

tion, we provide also that the exchanged correlation $\Delta\mathcal{C}$ as quantum resource of ergotropy, and we get a new explicative bounds on the ergotropy according to [16–18].

We analyzed the effect of the ergotropy of coherence and population and the free energies of coherence on the ergotropy bounds. We also express the global free energy of coherence for S in terms of the local coherences of S_{12} , C , and B , as well as the difference between the total and dephased mutual information, which gives a sense of the effect of correlation exchange between the subsystems.

IV. CONCLUSION

We have developed a theoretical framework to study the effect of structured reservoirs on the charging of a quantum battery through three different interaction scenarios.

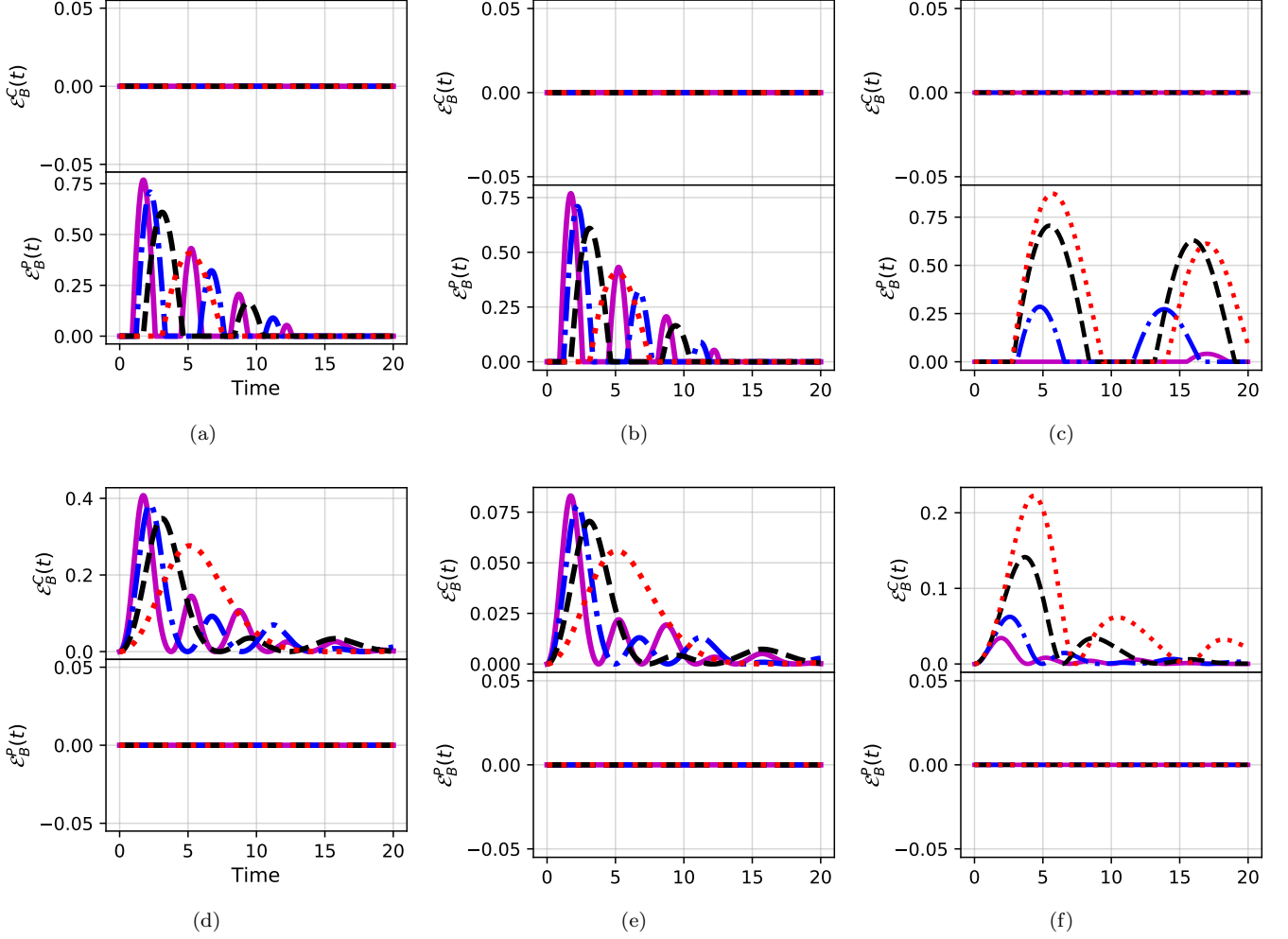


FIG. 4. Time evolution of $\frac{\mathcal{E}_B^C(t)}{\omega_B}$ and $\frac{\mathcal{E}_B^P(t)}{\omega_B}$, representing the ergotropy of coherence and population of the quantum battery, respectively. Panels (a)–(c) correspond to scenarios (I_a, II_a, III_a) , while panels (d)–(f) correspond to scenarios (I_b, II_b, III_b) . The coupling strength is varied as $g = 0.03, 0.05, 0.07$, and 0.09 (in units of ω_{S_2}), represented by red (dotted), black (dashed), blue (dot-dashed), and magenta (solid) curves.

Our analysis establishes coherence, populations, and correlation exchange as central resources governing the charging dynamics and the extractable work, and we provide the bounds on the ergotropy for each scenario.

Numerically we provide, for incoherent initial states, ergotropy originates solely from population, while coherent initial states enable additional contributions from coherence transfer and correlation backflow.

We derived analytical bounds on ergotropy in terms of the free energy of coherence and demonstrated their consistency with numerical simulations.

The interaction between structured reservoirs and autonomous charging dynamics highlights a mechanism for boosting quantum battery performance without external work. Our results extend previous approaches by explicitly incorporating structured environments and offer a pathway toward experimental realization in superconducting qubit platforms.

ACKNOWLEDGMENTS

A. KHOUDIRI acknowledges CNRST-Morocco support for this research within the Program "PhD-Associate Scholarship – PASS".

DECLARATION OF INTEREST

The authors declare that they have no conflict of interest.

DATA AVAILABILITY STATEMENT

No data statement is available.

-
- [1] Max F Riedel et al, "The European quantum technologies flagship programme", *Quantum Sci. Technol.* **2** 030501 (2017).
- [2] Antonio Acín et al, "The quantum technologies roadmap: a European community view", *New J. Phys.* **20** 080201 (2018).
- [3] J. Q. Quach, G. Cerullo, and T. Virgili, "Quantum batteries: The future of energy storage?," *Joule* **7**, 2195–2200 (2023).
- [4] A. Demir, E. Yildiz, and C. Kaya, "Application of quantum computing in the design of new materials for batteries," *J. Tecnol. Quantica* **1**, 288–300 (2024).
- [5] D. Farina, G. M. Andolina, A. Mari, M. Polini, and V. Giovannetti, "Charger-mediated energy transfer for quantum batteries: An open-system approach," *Phys. Rev. B* **99**, 035421 (2019).
- [6] G. M. Andolina, D. Farina, A. Mari, V. Pellegrini, V. Giovannetti, and M. Polini, "Charger-mediated energy transfer in exactly solvable models for quantum batteries," *Phys. Rev. B* **98**, 205423 (2018).
- [7] S. Elghaayda, A. Ali, S. Al-Kuwari, A. Czerwinski, M. Mansour, and S. Haddadi, "Performance of a superconducting quantum battery," *Adv. Quantum Technol.* **2025**, 2400651.
- [8] Z. G. Lu, G. Tian, X. Y. Lü, and C. Shang, "Topological quantum batteries," *Phys. Rev. Lett.* **134**, 180401 (2025).
- [9] B. Ahmadi, P. Mazurek, S. Barzanjeh, and P. Horodecki, "Super-optimal charging of quantum batteries via reservoir engineering," *Phys. Rev. Appl.* **23**, 024010 (2024).
- [10] F. Cavaliere, G. Gemme, G. Benenti, D. Ferraro, and M. Sassetti, "Dynamical blockade of a reservoir for optimal performances of a quantum battery," *Commun. Phys.* **8**, 76 (2025).
- [11] Y. Yao and X. Q. Shao, "Reservoir-assisted quantum battery charging at finite temperatures," *Phys. Rev. A* **111**, 062616 (2025).
- [12] B. Ahmadi, P. Mazurek, P. Horodecki, and S. Barzanjeh, "Nonreciprocal quantum batteries," *Phys. Rev. Lett.* **132**, 210402 (2024).
- [13] K. Xu, H. J. Zhu, G. F. Zhang, and W. M. Liu, "Enhancing the performance of an open quantum battery via environment engineering," *Phys. Rev. E* **104**, 064143 (2021).
- [14] J. L. Li, H. Z. Shen, and X. X. Yi, "Quantum batteries in non-Markovian reservoirs," *Opt. Lett.* **47**, 5614–5617 (2022).
- [15] M. Alimuddin, T. Guha, and P. Parashar, "Structure of passive states and its implication in charging quantum batteries," *Phys. Rev. E* **102**, 022106 (2020).
- [16] G. Francica, F. C. Binder, G. Guarnieri, M. T. Mitchison, J. Goold, and F. Plastina, "Quantum coherence and ergotropy," *Phys. Rev. Lett.* **125**, 180603 (2020).
- [17] A. Touil, B. Çakmak, and S. Deffner, "Ergotropy from quantum and classical correlations," *J. Phys. A: Math. Theor.* **55**, 025301 (2021).
- [18] T. Biswas, M. Lobejko, P. Mazurek, K. Jałowiecki, and M. Horodecki, "Extraction of ergotropy: Free energy bound and application to open cycle engines," *Quantum* **6**, 841 (2022).
- [19] R. Castellano, D. Farina, V. Giovannetti, and A. Acín, "Extended local ergotropy," *Phys. Rev. Lett.* **133**, 150402 (2024).
- [20] S. Lorenzo et al, "Composite quantum collision models", *Phys. Rev. A*, **96**, 032107 (2017).
- [21] H.-P. Breuer, F. Petruccione. "The theory of open quantum systems". Oxford University Press(2002).
- [22] A. Rivas Vargas, "Open quantum systems and quantum information dynamics", (Doctoral thesis, Universitaire Ulm) (2011).
- [23] S. Ghosh, A. Opala, M. Matuszewski, T. Paterek, and T. C. H. Liew, "Quantum reservoir processing," *npj Quantum Information* **5**, 35 (2019).
- [24] B. L. Fang, J. Shi, and T. Wu, "Quantum-memory-assisted entropic uncertainty relation and quantum coherence in structured reservoir," *Int. J. Theor. Phys.* **59**, 763 (2020).
- [25] N. Linden, S. Popescu, and P. Skrzypczyk, "How small can thermal machines be? The smallest possible refrigerator," *Phys. Rev. Lett.* **105**, 130401 (2010).
- [26] A. Khoudiri, A. El Allati, Ö. E. Müstecaplıoğlu, and K. El Anouz, "Non-Markovianity and a generalized Landauer bound for a minimal quantum autonomous thermal machine with a work qubit," *Phys. Rev. E* **111**, 044124 (2025).
- [27] M. Lostaglio, D. Jennings, and T. Rudolph, "Description of quantum coherence in thermodynamic processes requires constraints beyond free energy," *Nat. Commun.* **6**, 6383 (2015).
- [28] E. Chitambar and G. Gour, "Comparison of incoherent operations and measures of coherence," *Phys. Rev. A* **94**, 052336 (2016).
- [29] W. De Roeck and C. Maes, "Quantum version of free-energy-irreversible-work relations," *Phys. Rev. E* **69**, 026115 (2004).
- [30] T. Baumgratz, M. Cramer, and M. B. Plenio, "Quantifying coherence," *Phys. Rev. Lett.* **113**, 140401 (2014).
- [31] J. Majer, J. M. Chow, J. M. Gambetta, J. Koch, B. R. Johnson, J. A. Schreier, *et al.*, "Coupling superconducting qubits via a cavity bus," *Nature* **449**, 443–447 (2007).
- [32] L. DiCarlo, J. M. Chow, J. M. Gambetta, L. S. Bishop, B. R. Johnson, D. I. Schuster, *et al.*, "Demonstration of two-qubit algorithms with a superconducting quantum processor," *Nature* **460**, 240–244 (2009).
- [33] L. DiCarlo, J. M. Chow, J. M. Gambetta, L. S. Bishop, B. R. Johnson, D. I. Schuster, *et al.*, "Demonstration of two-qubit algorithms with a superconducting quantum processor," *Nature* **460**, 240–244 (2009).
- [34] D. C. McKay, S. Filipp, A. Mezzacapo, E. Magesan, J. M. Chow, and J. M. Gambetta, "Universal gate for fixed-frequency qubits via a tunable bus," *Phys. Rev. Appl.* **6**, 064007 (2016).
- [35] S. Zakavati, F. T. Tabesh, and S. Salimi, "Bounds on charging power of open quantum batteries," *Phys. Rev. E* **104**, 054117 (2021).
- [36] Y. Khelifi, A. El Allati, A. Salah, and Y. Hassouni, "Quantum heat engine based on spin isotropic Heisenberg models with Dzyaloshinskii–Moriya interaction," *Int. J. Mod. Phys. B* **34**, 2050212 (2020).
- [37] A. El Allati, K. El Anouz, M. H. B. A. Chakour, and S. Al-Kuwari, "Non-Markovian effects on the performance of a quantum Otto refrigerator," *Phys. Lett. A*

- 496**, 129316 (2024).
- [38] Y. Khlifi, S. Seddik, and A. El Allati, “Steady state entanglement behavior between two quantum refrigerators,” *Physica A* **596**, 127199 (2022).
 - [39] M. H. B. Chakour, A. El Allati, and Y. Hassouni, “Entangled quantum refrigerator based on two anisotropic spin-1/2 Heisenberg XYZ chain with Dzyaloshinskii–Moriya interaction,” *Eur. Phys. J. D* **75**, 42 (2021).
 - [40] B. M. H. Abdou Chakour, A. El Allati, and Y. Hassouni, “[Title not provided],” *Phys. Lett. A* **451**, 128410 (2022).
 - [41] Y. Khlifi, A. El Allati, A. Salah, and Y. Hassouni, “Evaluating the performance of a refrigerator by an external system using entanglement,” *Eur. Phys. J. D* **75**, 195 (2021).